Implementing and Evaluating Candidate-Based Invariant Generation

Adam Betts, Nathan Chong, Pantazis Deligiannis, Alastair F. Donaldson, Jeroen Ketema

Abstract—The discovery of inductive invariants lies at the heart of static program verification. Presently, many automatic solutions to inductive invariant generation are inflexible, only applicable to certain classes of programs, or unpredictable. An automatic technique that circumvents these deficiencies to some extent is *candidate-based invariant generation*, whereby a large number of candidate invariants are guessed and then proven to be inductive or rejected using a sound program analyser. This paper describes our efforts to apply candidate-based invariant generation in GPUVerify, a static checker of programs that run on GPUs. We study a set of 383 GPU programs that contain loops, drawn from a number of open source suites and vendor SDKs. Among this set, 253 benchmarks require provision of loop invariants for verification to succeed.

We describe the methodology we used to incrementally improve the invariant generation capabilities of GPUVerify to handle these benchmarks, through *candidate-based invariant generation*, whereby potential program invariants are speculated using cheap static analysis and subsequently either refuted or proven. We also describe a set of experiments that we used to examine the effectiveness of our rules for candidate generation, assessing rules based on their *generality* (the extent to which they generate candidate invariants), *hit rate* (the extent to which the generated candidates hold), *effectiveness* (the extent to which provable candidates actually help in allowing verification to succeed), and *influence* (the extent to which the success of one generation rule depends on candidates generated by another rule). We believe that our methodology for devising and evaluation candidate generation rules may serve as a useful framework for other researchers interested in candidate-based invariant generation.

The candidates produced by GPUVerify help to verify 231 of these 253 programs. An increase in precision, however, has created sluggishness in GPUVerify because more candidates are generated and hence more time is spent on computing those which are inductive invariants. To speed up this process, we have investigated four under-approximating program analyses that aim to reject false candidates quickly and a framework whereby these analyses can run in sequence or in parallel. Across two platforms, running Windows and Linux, our results show that the best combination of these techniques running *sequentially* speeds up invariant generation across our benchmarks by $1.17\times$ (Windows) and $1.01\times$ (Linux), with per-benchmark best speedups of $93.58\times$ (Windows) and $48.34\times$ (Linux), and worst slowdowns of $10.24\times$ (Windows) and $43.31\times$ (Linux). We find that *parallelising* the strategies marginally improves overall invariant generation speedups to $1.27\times$ (Windows) and $1.11\times$ (Linux), maintains good best-case speedups of $91.18\times$ (Windows) and $44.60\times$ (Linux), and, importantly, dramatically reduces worst-case slowdowns to $3.15\times$ (Windows) and $3.17\times$ (Linux).

Index Terms—formal verification; GPUs; invariant generation

1 Introduction

An *invariant* is a property that captures program behaviours by expressing a fact that always holds at a particular program point. Invariants are vital to static verification tools to reason about loops and procedure calls in a modular fashion [1], and this reasoning requires proving that invariants are *inductive*: in the case of loops this means that they hold on entry to the loop (the base case), and that if the invariants hold at the start of some arbitrary iteration of the loop, they are guaranteed to hold at the end of the iteration (the step case).

The automatic discovery of inductive invariants is a challenging problem that has received a great deal of attention from researchers [2], [3], [4], [5], [6], [7], [8], [9], [10], [11], [12]. A flexible solution is offered by *candidate-based invariant generation* [5], [13] whereby a large number of candidate invariants (henceforth, just *candidates*) are speculated through simple *rules* (e.g. based on patterns observed in the abstract syntax tree of a program) and are then checked using formal verification methods. The output is a subset of the candidates that can be proven to hold; if all candidates are rejected then the weakest invariant, i.e. `true`, is returned.

Although candidate-based invariant generation is popular in several static verification tools, no general methodology exists to implement and to evaluate such a framework. We address this problem in this paper by describing the systematic way in which we incorporated new rules into GPUVerify [14], a static verification tool for programs that have been designed to run on Graphics Processing Units (GPUs), and by proposing a set of questions that allow rules to be comprehensively evaluated, irrespective of the application domain. Our evaluation criteria broadly assess whether rules produce inductive invariants, whether there are dependencies among rules, and the extent to which rules help to verify programs.

We applied the proposed evaluation criteria to GPUVerify using a set of 383 GPU programs collected from a wide variety of sources. This endeavour led to three interesting discoveries. First, the rules as a whole have

• *A. Betts, N. Chong, P. Deligiannis, A.F. Donaldson and J. Ketema are with the Department of Computing, Imperial College London, London SW7 2AZ, UK.*
E-mail: {abetts,nyc03,p.deligiannis13,afd,j.ketema}@imperial.ac.uk

greatly increased the accuracy of GPUVerify, helping to verify 231 out of 253 GPU programs where loop invariants are required. Second, most rules in GPUVerify are independent of each other: if a rule produces inductive invariants, then the proof of those candidates can be established in isolation from inductive invariants of other rules. Third, some rules in GPUVerify are redundant because they no longer produce candidates that are essential to verify a single GPU program: they have been superseded by more general rules.

Increased precision, however, has come with a price: GPUVerify has become less responsive with the introduction of more rules because more candidates must be proven to be inductive invariants or rejected as false. In one specific case, a GPU program that verifies within 10 minutes *without* invariants cannot be verified in the same time frame due to the overhead of candidate-based invariant generation. To counter the performance lag, we have investigated four *under-approximating* program analyses whose aim is refute false candidates quickly, and we have devised a framework where several of these analyses can run either *in sequence* or *in parallel*. Evaluating these techniques on two different machines, running Windows and Linux, respectively, we discovered that:

- In the best case, accelerating Houdini using a sequential combination of techniques sped up invariant generation performance by $93.58\times$ (Windows) and $48.34\times$ (Linux).
- In the worst case, attempts at sequential acceleration did not pay off, slowing down invariant generation by $10.24\times$ (Windows) and $43.31\times$ (Linux).
- Over all benchmarks, sequential acceleration sped up invariant generation by $1.17\times$ (Windows) and $1.01\times$ (Linux).
- Parallelising our strategies maintained good best case speedups of $91.18\times$ (Windows) and $44.60\times$ (Linux), while reducing worst-case slow downs to $3.15\times$ (Windows) and $3.17\times$ (Linux). The key benefit of parallelisation here is that it prevents a runaway under-approximating analysis from severely delaying invariant discovery.
- Overall, parallelisation gave a marginally better speedup across our benchmarks, of $1.27\times$ (Windows) and $1.11\times$ (Linux).

The rather different results obtained for these distinct platforms emphasise the importance of accounting for measurement bias [15]: the operating system and programming language runtime used to conduct program analysis can have a noticeable impact on performance results.

In summary, our main contributions are:

1) An account of a systematic approach to manually deriving domain-specific rules for candidate-based invariant generation; while the rules are specific to the context of GPU kernel verification we believe the principled approach we have taken in their discovery can be transferred to other domains.
2) An experimental study of generality, hit-rate, worth and influence of these candidate generation rules; we believe the metrics we present, and our experimental method, will guide other researchers in evaluating candidate-based invariant generation techniques.
3) General strategies for accelerating candidate-based invariant generation via under-approximating program analyses, the application of parallel processing to combine multiple strategies, and a large experimental evaluation of these methods.

The remainder of the paper is structured as follows. Necessary background material is provided in Section 2. In Section 3, we outline some basic properties of the GPU programs in our evaluation set and describe how preconditions for each GPU program were procured. The methodology to implement and to evaluate candidate-based invariant generation appears in Section 4, and the measures undertaken to boost performance and an evaluation thereof are contained in Section 5. We survey related work in Section 6 and finish in Section 7 with our conclusions.

2 Background

This section has three parts. We begin, in Section 2.1, with a high-level overview of GPUVerify. Section 2.2 then motivates the need for inductive loop invariants. Finally, Section 2.3 briefly discusses the mechanics of candidate-based invariant generation.

2.1 GPU programs and GPUVerify

A GPU *kernel* is a computer program, typically written in CUDA [16] or OpenCL [17], that enables a general-purpose computation to be offloaded to a GPU. At run time, the kernel is launched with a thread configuration that specifies both the number of threads to run and the organisation of the threads in blocks of size `blockDim`, where the blocks form a grid of size `gridDim`. Each thread is parameterised by its thread and block identifiers (`threadIdx` and `blockIdx`), which allow it to compute memory addresses and make branch decisions. Threads have access to thread-private memory and memory regions that are shared at the block and grid level. Threads in the same block can communicate through shared memory using *barrier* operations.

GPU kernels are susceptible to data races and barrier divergence, which are programming errors. A *data race* occurs when two different threads access the same location in shared memory, at least one access is a write, and there is no intervening synchronisation. *Barrier divergence* happens when threads reach distinct syntactic barriers or when the same barrier is reached under divergent control flow. Proving that GPU kernels are free from these errors is the aim of GPUVerify [14], [18], [19].

The architecture of GPUVerify is depicted in Figure 1. GPUVerify begins by transforming a GPU kernel into a

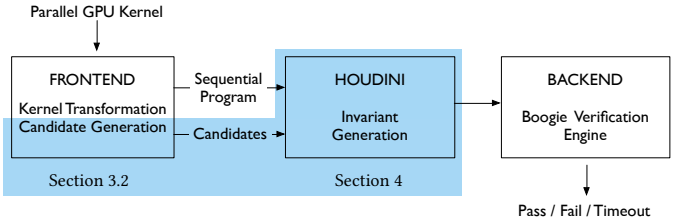

Fig. 1. The architecture of GPUVerify. The shaded parts of the pipeline—candidate generation and accelerating Houdini—are the focus of this paper.

```
                        assert φ;   // (base case)
                        havoc modset(B);
while (c)               assume φ;
invariant φ {           if (c) {
  B;                      B;
}                         assert φ; // (step case)
                          assume false;
                        }
```

Fig. 2. The loop-cutting transformation [23] used by GPUVerify. The loop on the left is transformed into the loop-free sequence of statements on the right.

sequential program (in the part labelled 'FRONTEND'); this is done in such a way that the correctness of the sequential program implies the data race- and barrier divergence-freedom of the GPU kernel. The transformation allows existing sequential verification techniques to be leveraged. GPUVerify's backend uses the Boogie verification engine [20] to verify the transformed kernel. Boogie calls upon an SMT solver, such as Z3 [21] or CVC4 [22], to check the verification conditions it generates.

GPUVerify is sound but incomplete: errors reported by the tool may be spurious (false positives). These false positives can be due to:

- abstract handling of floating-point operations,
- abstraction of the shared state, and
- insufficiently strong loop invariants.

In practice, we find that the last of these is the most common limitation of the tool. To combat this issue, GPUVerify uses candidate-based invariant generation.

2.2 Inductive loop invariants in GPUVerify

GPUVerify employs a *loop-cutting transformation* [1], [23] during the process of turning a GPU program into a verification condition. This approach transforms each loop into a loop-free sequence of statements that over-approximates the effects of the loop on the program state. To generate the replacement sequence, we need a property—a loop invariant—that holds each time the loop head is reached during execution.

The transformation is depicted in Figure 2: the input loop and its invariant ϕ on the left are turned into the loop-free sequence on the right. In the transformed

```
i := 0;
j := 0;

while (i < 100)
  invariant j = 2i;
  invariant j ≤ 200;
{
  i := i + 1;
  j := j + 2;
}

assert j = 200;
```

Fig. 3. An example code snippet annotated with loop invariants that allow proving the assertion $j = 200$.

sequence, the loop invariant is checked in two places. The first check ensures that the property is satisfied on entry to the loop (the base case), while the second check ensures the property is maintained by each execution of the loop body (the step case); if both can be proven, then the invariant is *inductive*. Observe that the step case requires the program to be in an arbitrary state which *already* satisfies the loop invariant; this establishes the induction hypothesis. The arbitrary state is obtained by assigning a non-deterministic value to each variable possibly modified in the loop body (using the `havoc modset(B)` statement), and then assuming the loop invariant (using the `assume` ϕ statement). If the loop guard evaluates to `true`, the step case then checks that no assertions can fail during execution of the loop body `B`, and that execution of the body results in a state that satisfies the loop invariant.

Example

To illustrate inductive loop invariants, consider the annotated code snippet in Figure 3, which repeatedly increments the variables i and j.

The first invariant, $j = 2i$, is inductive in isolation. The invariant holds trivially on entry to the loop when $i = j = 0$ (the base case), and is maintained by the loop body provided that the invariant and loop guard hold before the body executes (the step case):

$$j = 2i \ \wedge \ i < 100 \Rightarrow (j + 2) = 2(i + 1)\,.$$

The second invariant is *not* inductive in isolation since $j \leq 200$ and $i < 100$ do not imply $(j+2) \leq 200$. However, the invariant is inductive in conjunction with $j = 2i$:

$$j \leq 200 \ \wedge \ j = 2i \ \wedge \ i < 100 \Rightarrow (j + 2) \leq 200\,.$$

The two invariants together with the negation of the loop guard suffice to prove the assertion near the bottom of Figure 3:

$$j = 2i \ \wedge \ j \leq 200 \ \wedge \ i \geq 100 \Rightarrow j = 200\,.$$

2.3 Candidate-based invariant generation

GPUVerify employs candidate-based invariant generation to compute inductive loop invariants automatically. The technique speculates a finite set of potential invariants, called *candidates*, that must be checked to ensure that they are, in fact, true invariants. Checking is done by means of the Houdini algorithm [5], which returns the unique, maximal conjunction of candidates that form an inductive invariant (see [13] for a proof of this property). The conjunction may be over the entire set of candidates or over some subset, including the empty set (corresponding to the trivial invariant `true`). We provide some more details regarding the two phases of this approach.

2.3.1 Phase one: the guess phase

This phase supplies the candidates for a given program. Guessing is domain specific and is free to use any static, dynamic, or hybrid technique. A simple example is the use of syntactic checks that generate candidates based on pattern matching in the abstract syntax tree. Importantly, this phase can be aggressive, generating a large set of candidates: false candidates cannot introduce unsoundness because the Houdini algorithm (in the check phase) will simply refute them. Section 4 discusses the kinds of guesses performed by GPUVerify.

2.3.2 Phase two: the check phase

Beginning with a full set of candidates, Houdini removes candidates that cannot be proven, until a fixpoint is reached. A candidate may fail to be proven because the candidate is either false or non-inductive (corresponding to a base case or step case assertion failure in Figure 2). Either way, we refer to such a candidate as *false*.

Houdini is sound, deterministic, and terminating, assuming each call to the underlying SMT solver returns (which is not guaranteed if the logic used to encode verification conditions is undecidable). For single-procedure programs, such as those analysed by GPUVerify, the number of SMT solver calls is proportional to the number of candidates because Houdini only considers conjunctions of candidates.

Let us demonstrate Houdini using Figure 4, which gives a program that repeatedly cycles the values $1, 2, 3$ around the variables x, y, z. We assume the guess phase has speculated the candidates C_0 through C_6. Houdini must now compute the maximal inductive invariant that is a conjunction of a subset of these candidates. The figure shows how the set of candidates evolves during each iteration of the algorithm. During the first iteration, Houdini removes C_1 and C_3 because they are not true on loop entry (the base case). No further candidates can be removed during this iteration: in the base case all other candidates are true, and the step case holds vacuously because candidates C_0 and C_1, which are mutually inconsistent, are both assumed to hold. During the second iteration, the candidates C_0 and C_6 are refuted because they are not preserved by the loop. To see why C_6 is not preserved consider a state in which $x = 1$ and $y = z = 2$: this state satisfies C_6 on loop entry, but not after execution of the loop body. During the third iteration, the candidate C_4 is refuted. This candidate could not be removed until C_0 was removed since assuming C_0 allows C_4 to be preserved by the loop. This illustrates dependencies between candidates, where refutation of a specific candidate is only possible after refutation of certain other candidates. A fixpoint is reached during the final iteration: the remaining candidates, C_2 and C_5, form an inductive invariant, and Houdini returns $C_2 \wedge C_5$. It is worth noting that candidate C_6 is an invariant of the loop; it is refuted by Houdini due to not being inductive, as described above. If on the other hand additional candidates $x \neq z$ and $y \neq z$ were provided initially then, because they are mutually inductive, C_6 and the two new candidates would be returned by Houdini.

3 Benchmark suite

This paper studies invariant generation in GPUVerify using a set of 383 benchmarks collected from nine sources:

- 54 OpenCL kernels from the *AMD Accelerated Parallel Processing SDK* v2.6 [24],
- 98 CUDA kernels from the *NVIDIA GPU Computing SDK* v5.0 and v2.0 [25],
- 16 CUDA kernels hand-translated from Microsoft's *C++ AMP Sample Projects* [26],
- 20 CUDA kernels originating from the *gpgpu-sim* benchmarks [27],
- 15 OpenCL kernels from the *Parboil* suite v2.5 [28],
- 18 OpenCL kernels from the *Rodinia* suite v2.4 [29],
- 50 OpenCL kernels from the *SHOC* suite [30],
- 88 OpenCL kernels generated by the PPCG parallel code generator [31] from the *PolyBench/C* benchmarks v4.0a [32], and
- 24 OpenCL kernels from the Rightware *Basemark CL* suite v1.1 [33].

We refer to the above benchmarks as the *LOOP set*.

All of the above suites are publicly available except for *Basemark CL*, which was provided to us under an academic license. The collection covers all the publicly available GPU benchmark suites of which we were aware at the start of our study. The kernel counts do not include 330 kernels that we manually removed:

- 82 kernels are trivially race- and divergence-free because they are executed by a single thread.
- 10 kernels use either inline assembly, function pointers, thread fences, or CUDA *surfaces*, which GPUVerify currently does not support.
- 40 kernels are data-dependent (i.e. their control flow depends on array inputs to the kernel), which requires refinements of the GPUVerify verification method that cannot be applied automatically [34].
- 198 kernels are loop free and, hence, do not require invariant generation.

```
i := 0;
x := 1;
y := 2;
z := 3;

while (i < 10000)
  candidate C0 : i = 0;
  candidate C1 : i ≠ 0;
  candidate C2 : 0 ≤ i;
  candidate C3 : 0 < i;
  candidate C4 : i < 10000;
  candidate C5 : i ≤ 10000;
  candidate C6 : x ≠ y;
{
    temp := x;
    x := y;
    y := z;
    z := temp;
    i := i + 1;
}
```

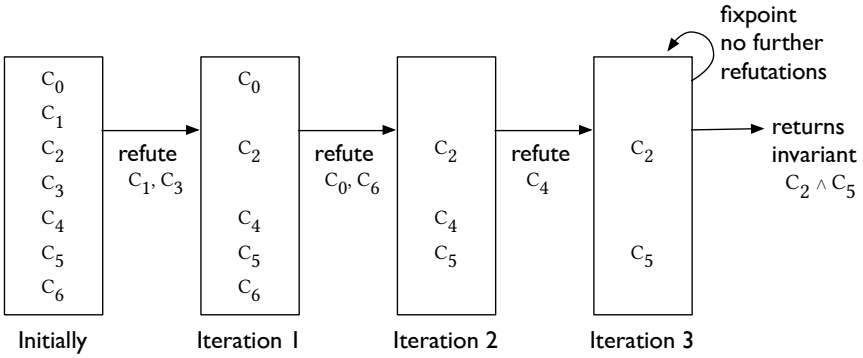

Fig. 4. An example program and a run of the Houdini algorithm, showing the candidates refuted at each iteration until a fixpoint is reached.

3.1 Loop properties

To discern the complexity of the kernels in the LOOP set, we counted the number loops and the loop-nesting depth of each kernel after full inlining had been applied.[1] Having many loops often makes a program hard to verify, and nested loops can be a particular challenge: in the case of a sequence of loops, proving that an invariant holds on entry to a given loop may only be possible if a sufficiently strong invariant is available for a preceding loop in the sequence; in the case where loop L_2 is nested inside loop L_1, invariants for L_1 may be required to prove that invariants of L_2 are inductive, and vice-versa.

We summarise the loop statistics in Table 1. The majority of kernels (68%) only feature a single loop or a pair of (possibly nested) loops, but there are still a significant number of kernels (122) containing a larger number of loops. At the very extreme, the `heartwall` kernel from the Rodinia suite features 48 loops that are syntactically distinct, i.e. they do not arise as a result of inlining.

Nested loops occur in 37% of kernels. Deep loop-nests are mostly found in the PolyBench/C kernels, with 42 of those kernels having a maximum loop-nest depth of three, and 9 having a maximum loop-nest depth of four. All kernels with a maximum loop-nest depth of five also originate from this set.

3.2 Obtaining scalar kernel parameters

Most kernels in the LOOP set are designed to be race free only for *constrained* thread configurations and input values. These preconditions are often implicit and very rarely documented, and any information that does exist appears as informal source code comments. Unfortunately, these preconditions must be communicated to GPUVerify in order to avoid spurious error reports.

TABLE 1
Basic loop statistics of the LOOP set.

Number of loops	1	2	3	4	5	6	7+
Kernels	168	93	52	34	19	2	15

Maximum loop-nest depth	1	2	3	4	5
Kernels	243	67	55	14	4

We solved the above problem by discovering constraints for kernel *scalar* parameters in the following way:

1) We ran the application in which the kernel was embedded and intercepted kernel calls using dynamic library instrumentation to note the input parameters of each kernel. For OpenCL applications we used KernelInterceptor [35]. For CUDA applications we used a similar prototype tool.[2]
2) We ran GPUVerify on the kernel in bug-finding mode, assuming the observed thread configuration but with unconstrained formal parameters. In bug finding mode, GPUVerify unrolls loops up to a fixed depth of two to avoid the need for loop invariants, thereby reducing the possibility of false positives. If GPUVerify reported a possible data race caused by an unconstrained *integer* parameter, then we restricted its value to the intercepted one. This step was repeated until GPUVerify was satisfied; in the extreme case this led to constraining all integer parameters.

We only added integer preconditions, because GPUVerify handles floating-point and array data abstractly.

1. GPUVerify performs full function inlining by default to increase verification precision. In practice this is possible because recursion and function pointers are prohibited in OpenCL and rare in CUDA.

2. https://github.com/nchong/cudahook

It is atypical for race freedom to require preconditions on floating-point inputs, while proving race freedom when this result depends on array preconditions requires manual methods (see the earlier discussion regarding kernels removed from our study).

The above process offers a pragmatic solution to garner a suitable but not overly constrained precondition, although the most general precondition may be missed. For example, in the case of the matrix transpose kernel of Figure 5 (to be discussed in Section 4.2), the process led to the precondition `height` $= 8$ being added for an 8×8 input matrix, instead of the more general `height` $=$ `gridDim.y` $\times$ `TILE_DIM`, which would allow us to also prove the kernel correct for matrices of different sizes.

After completing our study we reviewed the number of preconditions inserted using the above methodology (see Table 2). We found that 61% of kernels required preconditions, and on average each kernel required 1 precondition (with a standard deviation of 1.8). The largest number of preconditions required for a single kernel was 26 (for the `heartwall` kernel from the Rodinia suite).

TABLE 2
Number of introduced preconditions.

Preconditions	0	1	2	3	4	5	6	7	8+
Kernels	151	90	86	37	11	5	0	2	1

4 CANDIDATE-GENERATION IN GPUVERIFY

This section explains how we devised the rules that generate candidates in GPUVerify and evaluates whether these candidates increase the number of kernels that could be verified automatically. In Section 4.1 we describe the motivation, and our strategy for devising new invariant generation rules. In Section 4.2 we discuss, as an example, the intuition behind one of the rules that we developed (the remaining rules are outlined briefly in Appendix A). We then, in Section 4.3, assess the effectiveness of, and relationship between, the rules that we devised. During this process we discovered a number of defects in the GPU kernels we studied. We briefly document these issues in Section 4.4.

4.1 Process for deriving candidate-generation rules

To gauge the need for invariant generation in GPUVerify to prove absence of data races and barrier divergence, we attempted to verify each kernel in the LOOP set without loop invariants being either manually or automatically supplied. If a kernel verifies under these conditions then we say the kernel is *trivial*; typically, a trivial kernel has loops that either do not access the shared state at all, or that access shared arrays that are never written to by the kernel. We found 253 out of 383 (65%) kernels to be *non-trivial*, the majority of the LOOP set. Hence, assuming these kernels are indeed correct (and can be verified as such via suitable invariant annotations), invariant generation is crucial to the precision of GPUVerify.

The set of non-trivial kernels facilitated the design of new rules as follows:

1) We randomly picked a small number of kernels from the set, and manually determined a minimal set of loop invariants that enabled their verification.
2) Each picked kernel was updated to include the necessary loop invariants as *user-defined invariants*.
3) Common patterns were identified among the user-defined invariants that might apply in a wider setting. For each such pattern, we introduced a candidate-generation rule to GPUVerify.
4) We removed any user-defined invariants that were subsumed by the introduced rules.

We iterated the above process of invariant discovery until all kernels in the LOOP set—bar five kernels which we found to contain data races—could be verified automatically through a combination of invariants generated by our candidate-based approach and invariants provided manually (or, in the case of PolyBench/C, and as explained below, generated by a compiler). We rigorously applied step 4 above to ensure that all remaining user-defined invariants were necessary in order for verification to succeed using the candidate invariants generated by GPUVerify.

The sketched process led to the development of 19 rules, summarised in Appendix A. In Section 4.2 we explain how one such rule was developed.

Compiler-generated invariants for the PolyBench/C suite

The 88 kernels from the PolyBench/C suite were generated by PPCG [31], a polyhedral compiler equipped with a back-end that can compile polyhedral code, and some extensions thereof [36], into OpenCL.

Many of the machine-generated kernels feature a large number of loops, in some cases deeply nested due to the application of loop tiling program transformations. We verified a selection of these kernels by manually working out sufficient invariants, and found these invariants to be divided into two sorts: basic invariants about loop bounds (similar to invariants that were required by many other kernels) for which we had already devised suitable candidate-generation rules, and intricate, specialised invariants related to the memory access patterns associated with polyhedral code generation. For the latter invariants we worked with the lead developer of PPCG to add an option whereby the compiler can automatically generate a program-wide invariant characterising the access patterns of all loops. Adding the option was possible by virtue of the rich information about memory access patterns available in PPCG, which it uses to to perform code generation. The invariants generated by the compiler are independently checked by GPUVerify. For more details of this process, see [37].

By combining the compiler-generated invariants about access patterns with invariants inferred by GPUVerify relating to loop bounds it was possible to verify almost all

PolyBench/C kernels. Because the compiler-generated invariants are specific to this class of kernels, and because generation of the invariants by the compiler is reliable, we decided not to propose candidate-generation rules to speculate these invariants automatically. There were four kernels that did not verify out-of-the-box with this strategy. These kernels required invariants unique to them and, hence, we opted to supply these invariants manually.

4.2 Access breaking rule

As an illustrative example, we now describe a memory access pattern that we observed in a variety of the kernels, outline the process by which we manually derived invariants to characterise the access pattern, and comment on how these led to a candidate-generation rule that automates our manual process.

Consider the matrix transpose kernel of Figure 5, which is taken from the CUDA SDK [25]. The kernel reads from an input matrix `idata` of dimension `width` by `height` and writes to an output matrix `odata`. The matrices are stored in row-major order so an element $A_{x,y}$ of a matrix A is stored in a linear array at offset $x + \texttt{width} \times y$. The kernel is invoked with a 2-dimensional grid of 2-dimensional thread blocks. Each block is assigned a square tile of dimension `TILE_DIM` of the input and output matrices. Individual threads within a block stride along the assigned tile in increments of `BLOCK_ROWS`. During each iteration of the loop, each block of threads copies `TILE_DIM` by `BLOCK_ROWS` elements from `idata` to `odata`. For example, if the matrix dimension is 8×8, with $\texttt{TILE\_DIM} = 4$ and $\texttt{BLOCK\_ROWS} = 2$, then the kernel is invoked with a 2×2 grid of 4×2 blocks. Each block is assigned a tile of 4×4 elements. The read and write assignment of block $(1, 0)$ is shown on the right side of Figure 5. For example, thread $(1, 1)$ of block $(1, 0)$ assigns $\texttt{idata}_{1,5}$ to $\texttt{odata}_{5,1}$ and $\texttt{idata}_{1,3}$ to $\texttt{odata}_{3,1}$ when i equals 0 and 2, respectively.

Intuitively, GPUVerify checks for data race-freedom by analysing the intersection of read and write sets of all distinct thread pairs. In this example, the kernel is free from data races since `idata` is only ever read from, and distinct threads write to distinct offsets of `odata`. The loop invariants that we require must summarise the writes to `odata`. If W_t denotes the set of all writes that a thread t has issued, then a set of invariants that relates W_t to its thread identifiers is useful because two distinct threads must always have at least one block or thread identifier that is distinct:

$$\begin{aligned}\forall w \in W_t.\ ((w\ /\ \texttt{height})\ /\ \texttt{TILE\_DIM}) &= \texttt{blockIdx.x}\\ \wedge\ ((w\ /\ \texttt{height})\ \%\ \texttt{TILE\_DIM}) &= \texttt{threadIdx.x}\\ \wedge\ ((w\ \%\ \texttt{height})\ /\ \texttt{TILE\_DIM}) &= \texttt{blockIdx.y}\\ \wedge\ ((w\ \%\ \texttt{height})\ \%\ \texttt{TILE\_DIM})\ \%\ \texttt{BLOCK\_ROWS}&\\ = \texttt{threadIdx.y}&\end{aligned}$$

This invariant is trivially satisfied on loop entry because W_t is empty for all threads. To see that it is maintained by the loop consider an arbitrary write w from thread t to `odata`. The access will be of the form `index_out` + `i`, where `i` is a multiple of `BLOCK_ROWS`. Hence, w is:

```
(blockIdx.x × height × TILE_DIM)
  + (threadIdx.x × height)
  + (blockIdx.y × TILE_DIM)
  + threadIdx.y
  + i
```

which shows that the division and modulo operators as used in the invariant allow us to identify the thread t.

We refer to the above type of invariant as *access breaking* since the access pattern is broken down into the components identifying thread t. We have derived a candidate-generation rule to speculate access breaking invariants. For each memory access appearing in a kernel, we use cheap abstract syntax tree pattern-matching to determine whether the access uses thread identifiers. If so, then we trigger access breaking, which consists of rewriting the access expression to generate a possible equality for each of the components identifying a thread.

4.3 Evaluation of rules

GPUVerify presently has 19 rules for generating candidates—see Appendix A for a short description of each rule. Here we evaluate the effectiveness of these rules. In particular, we aim to provide answers to the following questions:

- Do the rules cause candidate invariants to be generated for a variety of kernels?
- To what extent do the rules produce true candidates?
- How often do true candidates generated by a rule prove to be essential for precise reasoning?
- To what extent are the rules independent, in terms of provability of the candidates they generate?
- For how many kernels does candidate-based invariant generation make the difference between verification succeeding or failing?

This set of questions, and our systematic approach to answering them experimentally, is one of the main contributions of our work: the questions and method easily generalise beyond our domain of GPU kernel verification, thus we believe they provide a framework that will be useful to other researchers interested in designing and evaluating candidate-based approaches to invariant generation.

4.3.1 Experimental setup

The experiments in this section were conducted on a machine with a 2.4GHz 4-core Intel Xeon E5-2609 processor and 16GB of RAM, running Ubuntu 14.04 and using CVC4 v1.5-prerelease, Clang/LLVM v3.6.2, and Mono v3.4.0. In GPUVerify, we enabled user-defined invariants and set the timeout to 30 minutes. We chose a large timeout so that more kernels could be explored, thus yielding a larger evaluation.

```
#define TILE_DIM 4
#define BLOCK_ROWS 2

__global__ void transpose(float *odata, float *idata,
                          int width, int height) {
  int xIndex = blockIdx.x * TILE_DIM + threadIdx.x;
  int yIndex = blockIdx.y * TILE_DIM + threadIdx.y;

  int index_in  = xIndex + width  * yIndex;
  int index_out = yIndex + height * xIndex;

  for (int i = 0; i < TILE_DIM; i += BLOCK_ROWS) {
    odata[index_out + i] = idata[index_in + i * width];
  }
}
```

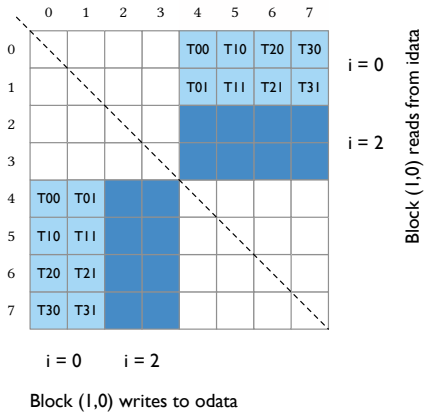

Fig. 5. A matrix transpose example taken from the CUDA SDK. The right side depicts reads of `idata` and writes of `odata` by block $(1, 0)$ for $\texttt{i} = 0$ and $\texttt{i} = 2$. Note that the reads and writes are not in-place over the same matrix.

TABLE 3
The number of kernels for which each rule triggers, and the hit rate and essentiality of each rule.

Rule	Kernels triggering a rule: Non-trivial	Trivial	Total	Hit rate	Essentiality
r0	70	0	70	74%	36
r1	204	7	211	89%	88
r2	30	0	30	83%	3
r3	30	0	30	60%	3
r4	85	7	92	59%	0
r5	141	6	147	99%	1
r6	81	3	84	100%	3
r7	46	0	46	91%	32
r8	184	6	190	75%	0
r9	238	17	255	47%	30
r10	143	6	149	87%	113
r11	46	0	46	91%	4
r12	103	0	103	49%	45
r13	114	2	116	52%	36
r14	50	5	55	40%	16
r15	50	5	55	29%	0
r16	46	0	46	4%	1
r17	14	0	14	4%	10
r18	7	0	7	90%	1

We removed 12 kernels from experiments reported upon in this section—unless indicated otherwise—leaving 372 kernels from the LOOP set. In the case of 11 of the 12 kernels, GPUVerify did not complete, even with the generous timeout of 30 minutes. In the case of one kernel GPUVerify ran out of memory.

4.3.2 Experiment: rule generality

Our first hypothesis was that the conditions under which a rule triggers would be found in a variety of non-trivial kernels but in few, if any, trivial kernels. To test this, we recorded, for each rule, the numbers of trivial and non-trivial kernels that contained at least one candidate produced by that rule.

Columns 2–4 of Table 3 displays the results. We see that the 130 trivial kernels rarely contain patterns that trigger a rule. This is positive because trivial kernels can be verified without the provision of any invariants, and checking the truth of superfluous candidates is likely to slow down the verification process. Overall, most rules are neither too speculative (rule r9 is activated by 255 kernels, the maximum) nor too bespoke (rule r17 is activated by 14 kernels, the minimum).[3] We believe this confirms that the process by which we introduced rules into GPUVerify has merit.

4.3.3 Experiment: rule hit rate

We further conjectured that a reasonable number of candidates produced by a rule would be true. We scrutinised this hypothesis by counting the following for each kernel in our evaluation set:

- the number of candidates produced by a rule, and
- the split between true and false candidates.

The *hit rate* of a rule is then the percentage of candidates that were true.

The results appear in the fifth column of Table 3. One rule (r6) has a hit rate of 100%, and five rules (r1, r5, r7, r11, r18) have hit rates close to 100%. We did not expect to find this many rules with such high hit rates because we designed our rules to guess candidates aggressively, in general preferring to err on the side of generating a large number of candidates (of which many may turn out to be false) to increase the chance of generating a true candidate in a scenario where it is needed for verification to succeed. Conversely, we see that rules r16 and r17 speculate poorly, indicating that the conditions under which they trigger should be refined. However, rule r17 would be in danger of becoming too specialised, as it is already unsuccessful at producing candidates for many kernels; the rule only triggers in 14 cases.

4.3.4 Experiment: rule worth

We cannot conclude from the previous experiment that rules with high hit rates are beneficial to verification.

3. We disregard rule r18 here, because the rule is tied to a particular GPUVerify command-line option that turns on an extension for awareness of warp-level synchronisation in CUDA [38], and can at most trigger for the 9 kernels in the LOOP set for which this option is enabled.

A devious rule can generate trivially true yet useless candidates for any kernel. Hence, we wanted to know whether rules produce constructive candidates that actually enable verification.

Our hypothesis was that there would be numerous kernels whose verification depended on the candidates generated by a particular rule, given that we engineered rules in response to non-verifying kernels. We tested this by observing whether GPUVerify reports differently for a kernel after a rule had been disabled. Specifically, we say that rule r is *essential* for a kernel if two conditions are satisfied:

1) the kernel verifies when *all* rules are enabled, and
2) disabling all candidates generated by rule r causes verification to fail or time out.

We counted the number of kernels for which each rule is essential.

The results are shown in final column of Table 3. The sum of the "essential" column is 422, meaning that there are 422 distinct (kernel, rule) pairs where the rule is essential for the kernel. Note that multiple rules may be essential for the same kernel.

At a glance, it may seem odd that rule r17 triggers for 14 kernels—and is essential for 10 of these—and yet only has a hit rate of 4%. The low hit rate is due to it being a measure of the generated candidates that are true invariants, and the particular rule generating many candidates per kernel.

Unessential rules (r4, r8, r15) are redundant and could be removed without affecting the precision of GPUVerify: they have been superseded by more general rules. It is possible that removal of these rules could change the *performance* of GPUVerify. This is because, for a given program, there are typically many ways to phrase a suitable set of invariants for verification, and the way the invariants are phrased can affect the ease or difficulty with which an underlying solver can process the resulting verification conditions.

4.3.5 Experiment: rule influence

Our final conjecture was that the rules were independent of each other, having been designed largely in isolation. To investigate this hypothesis, we observed whether disabling a rule in GPUVerify affected the hit rate of any of the other rules. In this case, we say that the disabled rule *influences* the rule whose hit rate changed.

Observe that if one rule influences another, then the hit rate of the second rule can only have decreased, because Houdini returns the unique, maximal conjunction of candidates forming an inductive invariant. To see this, consider the example from Section 2.2: the second invariant, $j \leq 200$, is only inductive in conjunction with the first, $j = 2i$. Hence, not speculating the first makes proving the second impossible.

The results of disabling each rule in turn in GPUVerify are represented in the heat map of Figure 6. For each pair of rules (r, s) we give the number of kernels where

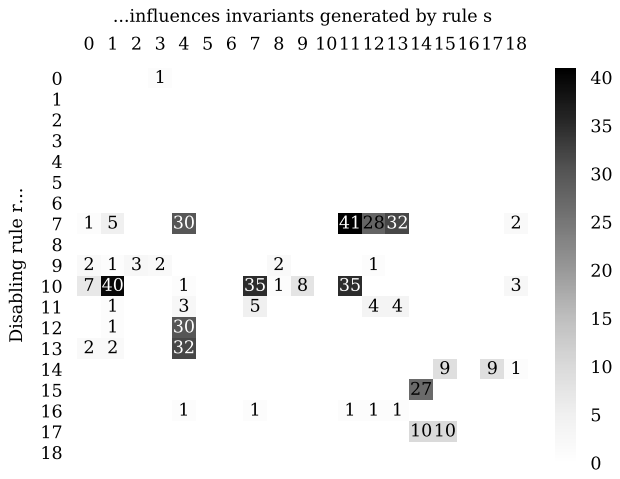

Fig. 6. For each pair of rules (r, s) the heatmap shows the number of kernels where rule r influenced rule s.

r influenced s. We see that the matrix is relatively sparse (with only 43 non-zero entries), which suggests that most rules do not influence each other. The major exceptions are rules r7 and r10, which speculate fundamental facts related to loop counters; these loop counters are likely to be used to index into shared arrays.

4.3.6 Experiment: overall increase in precision

An unanswered question is how much more precision is afforded by the rules as a whole. To answer this, we launched GPUVerify with all rules disabled and then with all rules enabled, and we counted the number of kernels that passed. Disabling all rules, 130 trivial kernels and 0 non-trivial kernels verified, whereas with all rules enabled, 129 trivial kernels and 231 non-trivial kernels verified, a net gain of 230 kernels. The slight drop in the number of trivial kernels verified is caused by a timeout: the rules hinder performance. We now turn our attention to this problem.

4.4 Defects detected during the process of deriving candidate-generation rules

The process of attempting to prove data race- and barrier divergence-freedom of a large set of kernels led us to discover that a number of the kernels we considered were in fact incorrect. We briefly detail the affected kernels and our efforts to report the defects we discovered in order for them to be fixed:

- A missing barrier was identified in the SHOC *sort* `top_scan` kernel. This race was reported and subsequently fixed.[4]
- Two threads writing to the same array location were identified in the CUDA 5.0 *convolutionFFT2D* `spPostprocess2D` kernel. This race was reported to Nvidia and is fixed in the CUDA 7.0 example set.

4. https://github.com/vetter/shoc/issues/30

- A missing barrier was identified in the Rodinia *SRAD* `reduce` kernel between the initialisation and use of an array. We reported this bug, and it has been fixed in version 3.1 of the suite.[5]
- Overlapping writes to an array due to an incorrectly set kernel parameter in the Rodinia *kmeans* `kmeans_swap` kernel. This has also been fixed in version 3.1 of the suite, in response to our report.
- Two threads writing to the same array location in the Rodinia *leukocyte* `dilate` kernel. This has also been fixed in version 3.1 of the suite, in response to our report.
- A similar issue in the Rodinia *particle filter* `normalize_weights_single` kernel, which has been reported and confirmed, but not yet fixed.
- A data race due to an incorrectly initialised vector in the Parboil *cutcp* benchmark, more specifically in the `opencl_cutoff_potential_lattice` kernel, which we have reported, with confirmation awaiting.
- What is technically a data race affecting several tests in the SHOC *DeviceMemory* benchmark; we have reported this, though because are tests for performance using random data the race may not be regarded as important.[6]

5 Accelerating Invariant Generation

As new rules were integrated into GPUVerify, the responsiveness of the tool diminished. To illustrate this, we ran a series of experiments over the LOOP set using the machine setup from Section 4.3.1, all with a per-kernel timeout of 10 minutes (all reported times are averages over five runs). During the first experiment we invoked GPUVerify with user-defined invariants *enabled* but all rules *disabled*. Then, for each subsequent experiment, we enabled successively more rules according to the order in which we implemented them. The final experiment therefore enabled all rules at our disposal. For each run, we recorded the times consumed by GPUVerify to process trivial and non-trivial kernels, including any timeouts. We split the measurements in this fashion to assess the effect of rule introduction on trivial kernels.

The results appear in Figure 7. The x-axis shows the evolution of the rules, and the two lines plotted show the evolution for the trivial and non-trivial kernels, respectively. We see that the introduction of rules approximately doubled the time needed to verify the trivial kernels. The overhead is caused by invariant generation, which GPUVerify must attempt for every kernel, trivial or otherwise. For non-trivial kernels, performance was hit by a modest $1.4\times$ slowdown. Merging the results reveals that almost two extra hours were needed to process all kernels in the LOOP set (from 233 minutes to 346 minutes) once all rules were integrated.

5. See acknowledgement at https://www.cs.virginia.edu/~skadron/wiki/rodinia/index.php/TechnicalDoc

6. https://github.com/vetter/shoc/issues/31

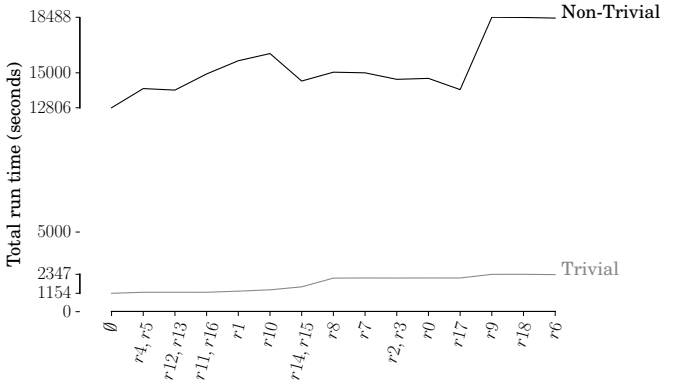

Fig. 7. The evolution of GPUVerify's performance.

We hypothesised that Houdini was the cause of the performance reduction. To validate this hypothesis, we measured the time spent at each GPUVerify stage, i.e. at each box in Figure 1, during the final experiment described above. The breakdown of times is as follows:[7]

- 482 seconds in the frontend (including candidate generation),
- 7781 seconds in Houdini, and
- 2180 seconds in the verification stage.

As anticipated, Houdini takes up the bulk (74%) of GPUVerify's run time. Motivated by this, we now consider techniques that accelerate candidate-based invariant generation.

Remark

The above experiment also allowed us to track the evolution of the number of kernels GPUVerify was able to verify. The results of this are shown in Figure 8. As before, the x-axis shows the evolution of the rules, and the two lines distinguish between there trivial and non-trivial kernels. The figure supports the hypothesis from Section 4.3.4 that rules r4, r8, and r15 were essential when introduced (although they no longer are at present).

5.1 Refutation engines

Our idea is to design a number of *under-approximations* of programs that are likely to kill candidates quickly. Here, a program T under-approximates a program S if the correctness of S implies the correctness of T, i.e. T can fail in the same or *fewer* ways than S.

Houdini employs an over-approximation of the input program—the loop-cut transformation exemplified in Figure 2—to compute an invariant from a set of candidates. Our idea is to design under-approximations of the loop-cut program that specialise in killing certain types of candidates. The correctness of our approach rests on a simple observation: any candidate that is shown to be false for an under-approximation of the

7. These numbers exclude 17 kernels as they exhausted the timeout.

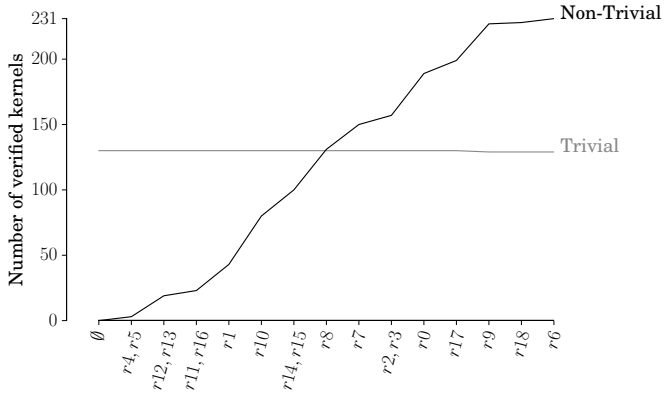

Fig. 8. The evolution of GPUVerify's verification capabilities.

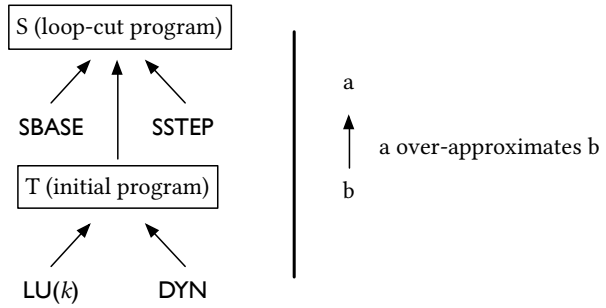

Fig. 9. Given an initial program T, Houdini operates on the loop-cut over-approximation S. We propose four refutation engines: variants of the loop-cut program that only check base cases (**SBASE**) and step cases (**SSTEP**)—both under-approximating S—and bounded loop unrolling for depth k (**LU(k)**) and dynamic analysis (**DYN**)—both under-approximating T.

loop-cut program must also be false for the loop-cut program itself. We use the term *refutation engine* to refer to an analysis that employs an under-approximation. With enough time, Houdini will eventually uncover all false candidates, thus a refutation engine is only useful if it finds false candidates ahead of Houdini or it allows Houdini to navigate a faster path through its search space. We have conceived four refutation engines that may meet this specification and which we investigate in the remainder of this section (see Figure 9 for a summary of the relationships between the engines).

5.1.1 Splitting loop checking: SBASE and SSTEP

Recall from Section 2.2 that the loop cutting transformation allows us to establish inductive invariants. As seen in Figure 2, the invariant must both hold on loop entry (the base case) and must be maintained by the loop (the step case). Omitting either of the assertions yields an under-approximation because the resulting program can fail in fewer ways than the original. This gives us two under-approximations of the loop-cut program S: one that only keeps the base cases (**SBASE**) and one that only keeps the step cases (**SSTEP**). We can also think of these under-approximations as splitting the program S into two subprograms (c.f. Figure 10). We speculate that refuting candidates in each subprogram separately may be faster than dealing with the program as a whole.

```
// base case
assert φ;
havoc modset(B);
assume φ;
if (c) {
  B;
  // step case omitted
  assume false;
}
```

```
// base case omitted
havoc modset(B);
assume φ;
if (c) {
  B;
  // step case
  assert φ;
  assume false;
}
```

Fig. 10. Splitting the loop checking for the loop-cut program S yields two under-approximations, **SBASE** (left) and **SSTEP** (right).

```
while (c)
  invariant φ {
  B;
}
```

```
if (c) {
  assert φ;
  B;
  if (c) {
    assert φ;
    B;
    if (c) {
      assume false;
    }
  }
}
```

Fig. 11. Bounded loop unrolling of the loop on the left for depth $k = 2$ yields the loop-free program on the right.

5.1.2 Bounded loop unrolling, LU(k)

Bounded loop unrolling a program for a given depth k yields a loop-free program where only the first k iterations of each loop are considered; when applied to a program T this yields an under-approximation of T. The method is commonly employed by bounded model checking tools such as CBMC [39]. Figure 11 shows the transformation of a loop after unrolling for depth $k = 2$. The loop-free fragment models k iterations of the loop. The resulting program is an under-approximation because it does not consider behaviours that require further loop iterations. The `assume false` statement implies that any execution that would continue past k iterations is infeasible and will not be considered [23].

Despite encoding only a subset of the original program's behaviour, loop unrolling leads to a syntactically larger program that, when converted to an SMT formula, may place a high burden on the underlying SMT solver. This is especially problematic in the case of nested loops, where unwinding an outer loop k times creates k copies of all inner loops, which must then be unwound in turn. For this reason, in our experiments we consider only the **LU(1)** configuration, where loops are unwound up to depth one.

5.1.3 Dynamic analysis, DYN

Executing a program T is a classic under-approximating analysis which, unlike our other refutation engines, is not dependent on a SMT solver. Instead, the statements of T are simply interpreted. To enable execution, we implemented an interpreter for *Boogie*—the intermediate verification language into which GPUVerify translates kernels and in which it expresses candidate invariants.[8]

Our dynamic analyser executes each kernel multiple times. On each fresh invocation, values for formal parameters and thread and block identifiers (i.e. `threadIdx` and `blockIdx`) are chosen that satisfy the preconditions of kernel (c.f. Section 3.2). Re-invocation halts once a selected coverage criterion—basic block coverage—is met or a specific number of launches has been reached. For many kernels we find that a *single* execution suffices to achieve full basic block coverage, because GPU code is rarely control dependent on formal parameters or thread variables. This means we can simply choose random values and can ignore sophisticated test-generation techniques, but this method is clearly not applicable to other domains. In spite of this simplicity, dynamic analysis may still be slow, for two reasons.

First, much execution time may be spent in loops with large loop bounds without refuting more candidates. Typically, this is due to dynamic analysis rejecting a candidate on the *first* loop iteration, or not at all. Hence, iterating through loops does not serve our aim of accelerating invariant generation. Our pragmatic solution is to bound the number of loop iterations summed across all loops. The downside is that a single loop may hog all the execution, preventing analysis of candidates in other loops. This drawback is more severe if there are candidates in loops after the cut-off point that are easily disproven through dynamic analysis but difficult to reject through an SMT-based refutation engine.

Second, candidates involving reads from and writes to arrays should be evaluated for all array indices discovered during the dynamic analysis. For instance, suppose we have arrays A and B and a candidate that asserts all accesses into A and into B are distinct. Then, we must evaluate this candidate with respect to all tuples (a, b), where a and b are *observed* array indices of A and B, respectively. Checking all tuples, however, is generally not feasible as the number grows exponentially in the length of the tuple. Instead, we select a constant number of random tuples, using the rationale that a candidate is likely true if it holds for this restricted subset. An obvious disadvantage is that the random selection may miss an instance that falsifies the property.

5.2 Evaluation of refutation engines

We conducted several experiments to address the following questions:

- Is a refutation engine able to reject candidates?
- Do refutation engines complement each other?
- Is invariant generation accelerated by a refutation engine?
- Does launching multiple refutation engines in parallel yield discernible gains?

5.2.1 Experimental setup

For these experiments we were interested in measuring the performance of GPUVerify using various invariant generation strategies. As the issue of performance fluctuation across platforms is well-known, we performed the experiments across two machines running different operating systems; this to reduce measurement bias [15]:

- a *Windows* machine with a 2.4GHz 4-core Intel Xeon E5-2609 processor and 16GB of RAM, running Windows 7 (64 bit) and using CVC4 v1.5-prerelease, Clang/LLVM v3.6.2, and Common Language Runtime v4.0.30319; and
- a *Ubuntu* machine also with a 2.4GHz 4-core Intel Xeon E5-2609 processor and 16GB of RAM, running Ubuntu 14.04 and using CVC4 v1.5-prerelease, Clang/LLVM v3.6.2, and Mono v3.4.0 (the same machine as used in the precision experiments).

The four refutation engines considered were **SBASE**, **SSTEP**, **LU(1)**, and **DYN**. The dynamic analyser had the following settings (c.f. Section 5.1.3): it quit as soon as 100% basic block coverage was met or 5 fresh executions completed; it terminated a single execution if 1,000 loop iterations were processed; and, every candidate referring to tuples of array indices was evaluated with respect to 5 of these. All these experiments included our user-defined invariants (the PolyBench/C suite also included the compiler-generated invariants discussed in Section 4.1), and used a timeout of 10 minutes. All reported times are averages over five runs.

5.2.2 Experiment: refutation engine power

The first hypothesis we wished to validate was whether every refutation engine could reject candidates at least as fast as Houdini. To this end, we ran each refutation engine in isolation and measured both the time consumed and the number of candidates refuted. We present the results in Table 4, showing numbers for Houdini (denoted by **H**) for comparative purposes.

The yardstick in this experiment is throughput, the number of refutations per second. We see that **DYN** is extremely effective on Windows, with a throughput that is four times that of the next highest, but much less so on Ubuntu, where the difference to the next highest is marginal. The throughputs of the other refutation engines appear mostly insensitive the machine setup; we attribute the discrepancy in **DYN** throughputs to differences in the Common Language Runtime implementation. **SBASE** has a high throughput on both machines and is much more effective than **SSTEP**, suggesting that it is easier for the SMT solver to reason about base case

8. Boogaloo [40] and Symbooglix [41] also support Boogie interpretation, but are generic and do not exploit knowledge specific to GPU kernels, as we do.

TABLE 4
Refutation engine performance and throughput.

Engine	Windows Refutations	Windows Total time (sec)	Windows Throughput (refutations/sec)	Ubuntu Refutations	Ubuntu Total time (sec)	Ubuntu Throughput (refutations/sec)
H	5703	17805	0.32	5615	15544	0.36
SBASE	3692	5053	0.73	3692	4991	0.74
SSTEP	3421	15125	0.23	3430	14664	0.23
LU(1)	3712	10096	0.37	3754	9541	0.39
DYN	2367	811	2.92	2301	2828	0.81

TABLE 5
Refutation engine similarity in terms of refuted candidates; a low Jaccard index indicates that two engines are complementary in their refutation power

Refutation engine pair		Windows Jaccard index	Ubuntu Jaccard Index
DYN	**SBASE**	0.12	0.17
DYN	**SSTEP**	0.23	0.25
DYN	**LU(1)**	0.22	0.25
SBASE	**SSTEP**	0.33	0.39
SBASE	**LU(1)**	0.63	0.70
SSTEP	**LU(1)**	0.49	0.53

candidates. **LU(1)** has a moderate throughput, but kills the most candidates among the refutation engines.

5.2.3 Experiment: complementary power

Our expectation was that refutation engines would each specialise in killing candidates generated by different rules, and that the refutation engines would therefore complement each other. To test this, we recorded the set of candidates rejected by a refutation engine across the *whole* LOOP set and then calculated the Jaccard index [42] between the sets for every pair of refutation engines. The Jaccard index numerically evaluates the similarity among sets:

$$J(A,B) = \frac{|A \cap B|}{|A \cup B|}\,.$$

For non-empty sets A and B, $J(A,B) = 1$ if the sets are identical, and $J(A,B) = 0$ if the sets share no common elements. The higher the Jaccard index, the more related the sets are. In our case, when comparing the sets of candidates killed by two distinct refutation engines, a low Jaccard index indicates that two engines are complementary in their refutation power.

Table 5 gives the Jaccard indices. We observe that **DYN** complements every SMT-based refutation engine, especially **SBASE**. Given that **DYN** and **SBASE** were also highest placed in the throughput experiment, we hypothesised that these refutation engines together are able to accelerate invariant discovery (we further investigate this hypothesis in the next section). Finally, the higher Jaccard index for **SBASE** and **LU(1)** suggests that these engines refute similar candidates, while the lower Jaccard index for **SBASE** and **SSTEP** indicates, as expected, that these engines target different candidates.

Note that the computed Jaccard indices differ between our experimental machines because of our use of a timeout; with enough time, our refutation engines would compute the same results on both platforms.

5.2.4 Experiment: overall performance impact

A drawback of evaluating a refutation engine in terms of throughput is that this disregards the difficulty in refuting the remaining false candidates. If a refutation engine merely quashes easily disproven candidates, then Houdini must still do the heavy lifting. The experiment described in this section therefore assesses whether the proposed refutation engines, or a combination thereof, actually help Houdini to reach a fixpoint faster.

We compared the time to return an invariant for a kernel across various refutation engine configurations. Our baseline configuration was Houdini *in isolation*, which is consistent with the current state of the art. We setup a number of *sequential* configurations whereby Houdini ran after a refutation engine had terminated; these configurations are denoted $\mathbf{R};\mathbf{H}$ where $\mathbf{R} \in \{\mathbf{DYN}, \mathbf{SBASE}, \mathbf{SSTEP}, \mathbf{LU(1)}\}$. We also considered a single *parallel* configuration whereby **DYN** and **SBASE** were launched alongside Houdini; this configuration is denoted $\mathbf{DYN}\|\mathbf{SBASE}\|\mathbf{H}$. We selected **DYN** and **SBASE** for our parallel configuration because of their high throughputs and complementary nature, as observed in our previous experiments.

In the parallel configuration, there is a shared pool of refutations that Houdini reads on each iteration. The exchange of rejected candidates is therefore *asynchronous*. An asynchronous exchange is allowed for two reasons:

1) Houdini guarantees that the number of candidates decreases in a strictly monotonic fashion [43], and
2) every candidate killed by a refutation engine may be trusted (because the engine employs an under-approximating analysis).

Note that the completion time of the parallel configuration is measured as the time for Houdini to terminate; at that point the refutation engines may still be running, but an invariant has been computed.

Figures 12 and 13 present the results for the Windows and Ubuntu machine, respectively. There are two types of bar charts. The first type (Figures 12a and 13a)

provides a birds-eye view of performance, showing the total times to process all kernels in the LOOP set for each configuration. The second (Figures 12b–12f and 13a–13f) narrows the focus to a specific configuration, grouping per-kernel performance comparisons into five intervals: $(-\infty, -2)$ (noteworthy slowdowns), $[-2, -1)$ (modest slowdowns), $[1, 1]$ (break-evens), $(1, 2]$ (modest speedups), and $(2, \infty)$ (noteworthy speedups). Each of these intervals is divided into two categories depending on whether we deem a kernel to be inherently *fast* (≤ 2 seconds for the baseline configuration to finish) or inherently *slow* (> 2 seconds for the baseline configuration to finish). We split the intervals to be able to evaluate whether the speedups and slowdowns of a configuration are actually noticeable to a user. Any improvement in speed is likely more noticeable for a slow kernel while, conversely, any performance deterioration is likely more so for a fast kernel. The threshold of two seconds is simply based on our experience to date.

We examine the results of the configurations in the following order: dynamic analysis, the SMT-based refutation engines, and the parallel setup.

Sequential configuration ***DYN*;*H***

On the Windows machine there was a noticeable boost in performance using the **DYN**;**H** configuration (compared to the baseline **H**). The overall run time improved from 17,806 to 15,283 seconds. The maximum 93.58× speedup enabled the invariant generation for the kernel exhibiting this speedup to finish within 6.41 seconds rather than timing out after 600 seconds.

Slowdowns become severe when a refutation engine is unable to kill any candidates, in which case sequential composition always reduces performance. For dynamic analysis, the magnitude of deceleration is generally dominated by the time required to interpret the loop body with the longest execution time. Indeed, the 3.19× slowdown occurred in the case of a kernel whose loop body has a large number of statements, taking invariant generation from 22.21 to 70.77 seconds. This shows that our heuristics to exit dynamic analysis early are not a panacea. We believe a more valuable solution would be to start dynamic analysis only if a coarse estimate of kernel execution time falls below a certain threshold. Nevertheless, this configuration offered the most impressive return: only 8 kernels suffer a noteworthy slowdown, none on inherently fast kernels, and the majority of kernels (202) benefited from a performance boost, 42 of which are noteworthy.

The picture is radically different on the Ubuntu machine, with a significant maximum slowdown and an overall loss in performance (16,632 instead of 15,544 seconds). Investigating the kernel for which the maximum slowdown occurs in more detail, we found that, on the Windows machine, **H** and **DYN**;**H** completed in 11.31 and 27.04 seconds, while, on the Ubuntu machine, the configurations completed in 7.49 and 324.33 seconds. The wide disparity between times cannot be attributed to variations in execution paths during dynamic analysis, because the kernel is *not* control dependent on formal parameter values or thread identifiers. Moreover, recording the dynamic statement count, we verified that the interpreter performs the same work on both machines—the counts matched (110,907 statements). The slowdown is therefore a consequence of statement execution time and ultimately how the Common Language Runtime is implemented; reaching the same conclusion as in our throughput experiment. In spite of this handicap, **DYN**;**H** still offered the best speedup, the second most speedups (184; after the **DYN**‖**SBASE**‖**H** configuration), and the most noteworthy speedups.

Our observations of dramatically different results between platforms emphasises the importance of accounting for measurement bias when conducting experimental studies [15], which we have attempted to do by reporting experiments on machines with different operating systems and runtime implementations.

Sequential configurations {***SBASE***, ***SSTEP***, ***LU(*1*)*** };***H***

SBASE;**H** is the only sequential configuration that offered an average cross-platform performance boost (17,428 instead of 17,806 seconds on the Windows machine, and 15,333 instead of 15,544 seconds on the Ubuntu machine).

SSTEP;**H** offered very little, consuming the most time on both machines, amassing the fewest speedups on both machines and creating the worst slowdown on the Windows machine.

LU(1**)**;**H** is similar to **SBASE**;**H** except that the former resulted in a few extra noteworthy speedups and a better maximum speedup on both machines, while the latter resulted in more speedups in total and consumed less time overall. Given that the throughput of **SBASE** was approximately double that of **LU(**1**)**, these results suggest that **LU(**1**)** kills more valuable candidates, leaving Houdini with less work to do. The work that **SBASE** undertakes is still worthwhile (every discovered false candidate is valuable), but it leaves Houdini with the more challenging false candidates.

Finally, we note that all of the SMT-based configurations negatively impacted the majority of fast kernels on both the Windows and Ubuntu machine. Hence, these refutation engines should only be enabled when GPUVerify suspects Houdini will struggle with the kernel and its candidates.

Parallel configuration ***DYN*‖*SBASE*‖*H***

In comparison to the other configurations, there was a marked improvement in average performance for the **DYN**‖**SBASE**‖**H** configuration, with a 1.27× speedup on the Windows machine and a 1.11× speedup on the Ubuntu machine. This met our expectation that execution of Houdini in parallel with the most powerful refutation engines is superior to Houdini in isolation.

Some of the other results, however, appear counterintuitive. We might expect parallelisation to completely

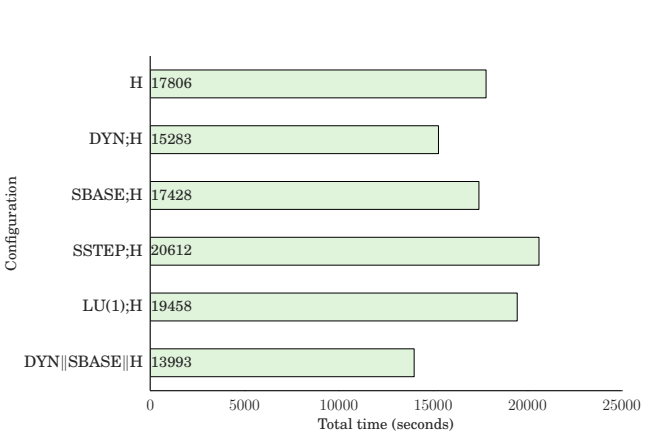

(a) Total run times

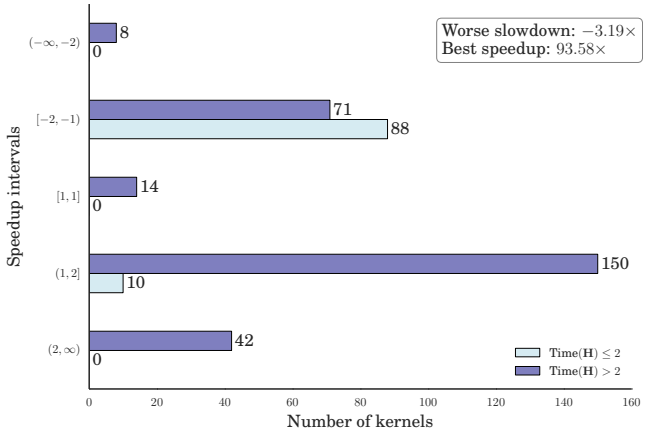

(b) **DYN;H**

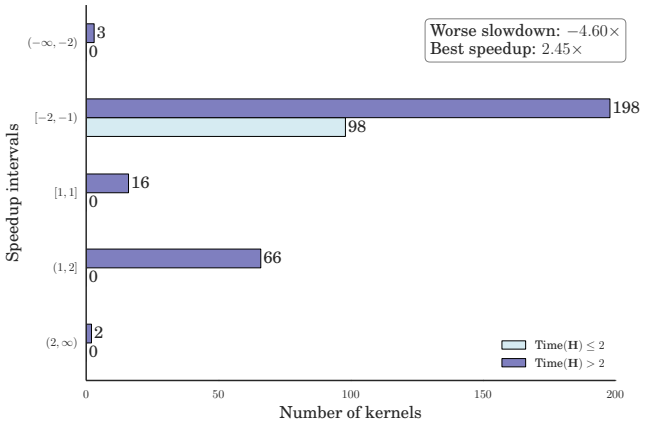

(c) **SBASE;H**

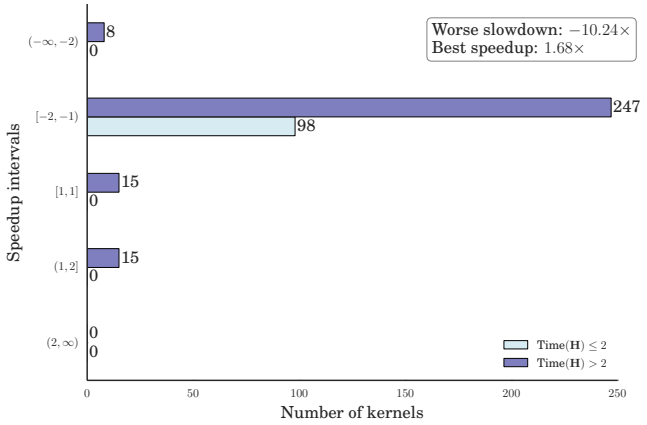

(d) **SSTEP;H**

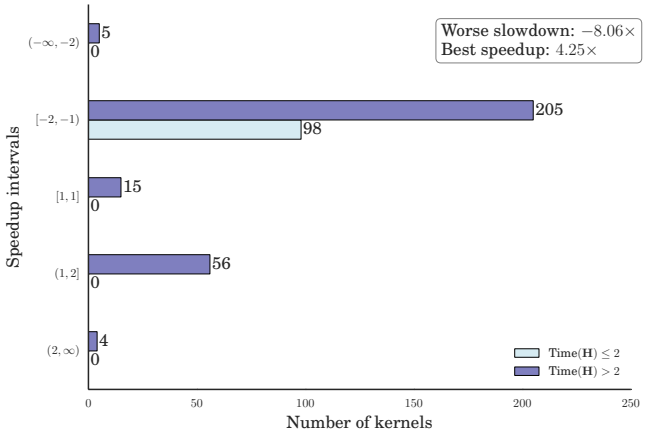

(e) **LU(1);H**

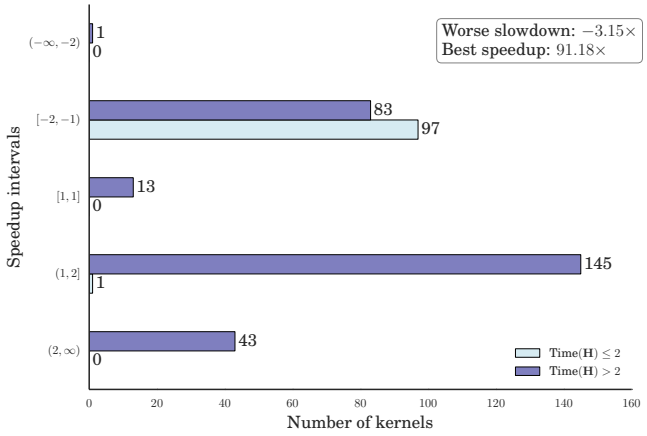

(f) **DYN||SBASE||H**

Fig. 12. Overall performance impact on the Windows machine.

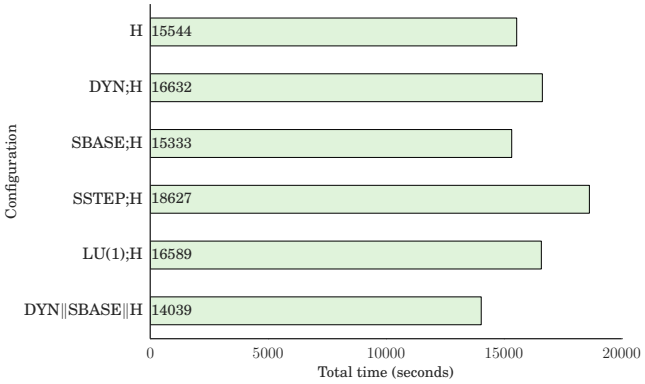

(a) Total run times

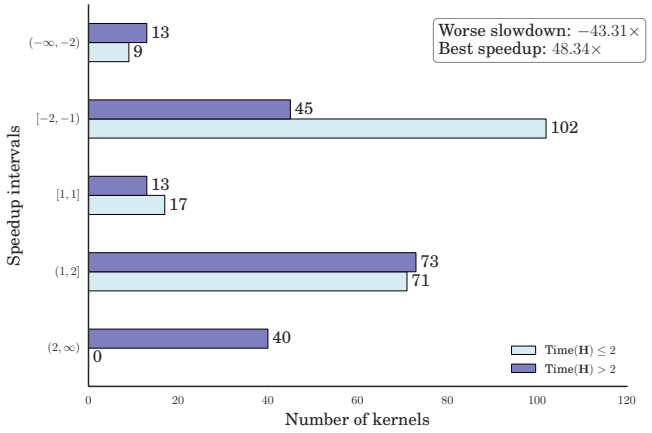

(b) **DYN;H**

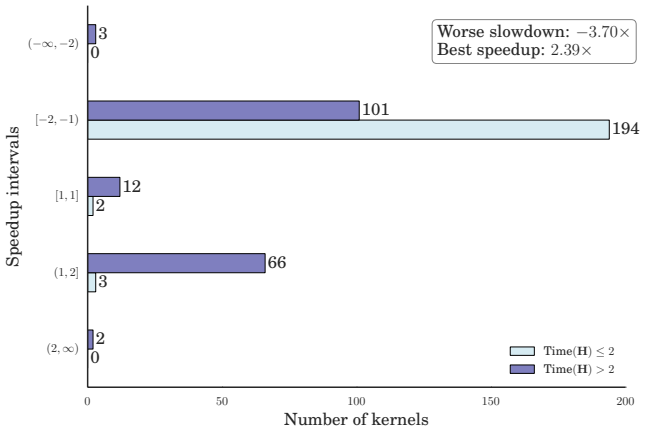

(c) **SBASE;H**

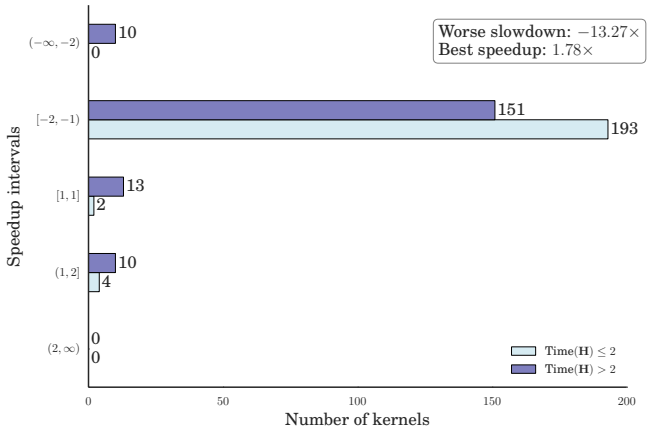

(d) **SSTEP;H**

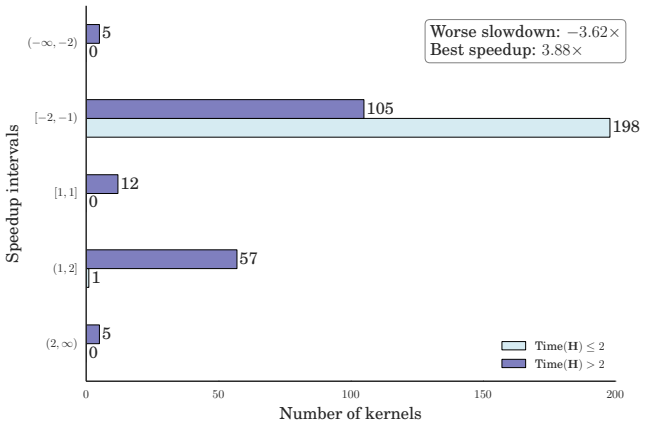

(e) **LU(1);H**

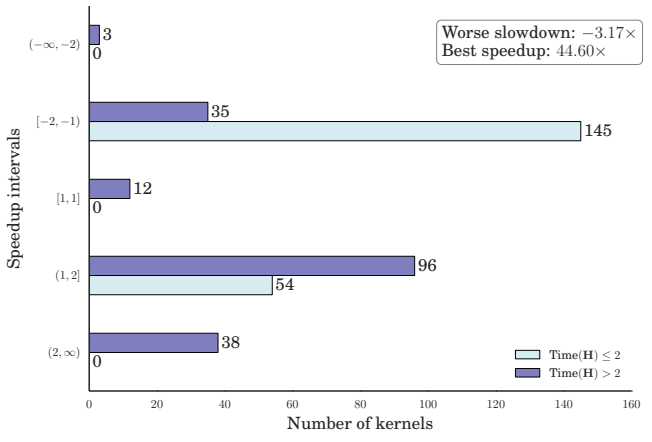

(f) **DYN||SBASE||H**

Fig. 13. Overall performance impact on the Ubuntu machine.

eliminate the possibility of multiple strategies slowing down invariant generation: modulo experimental error and the modest overheads of parallelism, it might seem that the performance of regular Houdini should be an upper bound on parallel performance. However, we find that worst-case slowdowns are reduced (from $3.19\times$ to $3.15\times$ on Windows, and from $43.31\times$ to $3.17\times$ on Linux), but not eliminated. The issue is that Houdini is not impervious to the other refutation engines: *how* the fixpoint is reached is influenced by the order in which refutations are discovered, and alternate orderings create variations in processing time. The same reason explains why **DYN**;**H** yields more speedups and a better maximum speedup on both machines.

6 Related work

Invariant generation has been a long-standing challenge in computer science, leading to many research works, e.g. [2], [3], [4], [5], [6], [7], [8], [9], [10], [11], [12] (by no means an exhaustive list). We discuss the works most closely related to our study.

6.1 Candidate-based invariant generation

Houdini was proposed as an annotation assistant for the ESC/Java tool [5], and is formally presented in [13]. The method is analogous to an invariant strengthening technique for circuit equivalence checking [6]; we believe the methods were discovered independently. Houdini can be viewed as a special instance of predicate abstraction [44], restricted to conjunctions of predicates. This restriction is what makes the runtime of Houdini predictable, involving a worst case number of solver calls proportional to the number of candidates. The restriction also makes it impossible to synthesise disjunctive invariants over predicates using Houdini. A recent compelling application of Houdini is in the Corral reachability checker, where Houdini is used to generate procedure summaries which in turn are used to guide search for bugs [45].

6.2 Abstract interpretation

Abstract interpretation [4] is a general program analysis framework that can be parameterised to generate inductive invariants over a given abstract domain. For instance, the Interproc analyser synthesises invariants over the abstract domain of linear inequalities, using the Apron library [7]. Predicate abstraction is abstract interpretation over the domain of Boolean combinations of predicates [46], and Houdini is thus a form of abstract interpretation where the domain is restricted to conjunctions of predicates. The main disadvantages of abstract interpretation are that it is inflexible, in the sense that generation of invariants beyond a given abstract domain requires a bespoke new domain to be crafted, and that to ensure convergence to a fixpoint it is necessary to apply *widening* which can be hard to control in a predictable manner. In contrast, a Houdini-based approach can easily be "tweaked" by adding new candidate generation rules on an example-driven basis, as we have demonstrated in this paper. Convergence to a fixpoint is also predictable based on the known set of candidates. In recent work, *Abstract Houdini* has been proposed in an attempt to combine the benefits of abstract interpretation and candidate-based invariant generation [8].

6.3 Invariant generation for affine programs

There has been significant progress recently on invariant generation for a restricted class of programs that operate on unbounded integers and only compute affine expressions over program variables. Under these restrictions, novel applications of Craig interpolation [9], abduction [10] and abstract acceleration [11] have been shown to be effective in invariant synthesis. The weakness of these methods are the restrictions on input programs. In our application domain, for example, programs operate on fixed-width bit-vectors and floating point numbers. It is necessary to reason precisely about bit-vectors to capture arithmetic using powers-of-two, frequently encoded efficiently using shifting and masking, and we require support for uninterpreted functions to abstract floating point operators but retain their functional properties. Furthermore, GPU kernels frequently exhibit non-linear computations. For example, reduction operations involve loops in which a counter exponentially varies in powers of two between an upper and lower bound. These characteristics render methods for affine programs inapplicable in our setting.

6.4 Dynamic invariant generation

The techniques discussed above all use static analysis to establish program invariants with certainty. In contrast, dynamic invariant generation, pioneered by the Daikon system [12] employs dynamic analysis with respect to a test suite to speculate *likely* invariants: facts that are found to hold invariantly during testing, with statistical evidence that these dynamic invariance of these facts appears to be non-coincidental. This method provides no guarantee that the suggested facts are actually true invariants. A study combining the Daikon method with extended static checking for Java considered the use of dynamically generated invariants as a source of candidates for Houdini [47].

6.5 Studies on invariant generation

A related study on invariant generation aimed to evaluate whether it is better to rely on manual effort, automated techniques or a combination of both in generating program invariants [48]. The study concludes that a combination is required: they found that Daikon inferred $5\times$ as many invariants as were written manually, but could only find approximately 60% of the manually

crafted invariants. Their benchmark set consisted of 25 classes taken from widely used libraries or written by students. The size of their benchmark set allowed them to investigate each inferred assertion individually; this is not feasible in our study due to the substantially larger number of benchmarks.

7 Conclusions

In this study we have shown that candidate-based invariant generation is valuable to GPUVerify, significantly increasing the precision of the tool and, to some extent, relieving the burden of manual loop-invariant discovery. This success is in large part due to our strategy of incorporating new rules into GPUVerify because candidate-based invariant generation is only as good as the supply of speculated candidates. However, our evaluation also provides a cautionary tale: rules may become redundant over time, particularly when new rules are introduced, thus a continual assessment of their use to the verification tool is worthwhile.

The wider issue with candidate-based invariant generation is that, in general, more rules mean more candidates and, ultimately, more processing time. The refutation engines and the infrastructure that we implemented to curb processing time proved effective when comparing invariant discovery with and without these techniques. Our mechanism to choose between refutation engines and between sequential or parallel processing mainly rested on empirical evidence of throughput and complementary power. The drawback of this, as the results indicate, is that the unselected refutation engines or processing mode can be better for *specific* kernels. As such, our setup ignores all properties of the program and of the candidate invariants. Future work may therefore investigate machine learning techniques to fine-tune the setup.

Appendix A
Invariant generation rules in GPUVerify

Rules broadly fall into the following categories:

- Patterns over accesses. These summarise reads and writes that are issued by the execution of a loop. Examples include strides or ranges of accesses and can include one, two or three-dimensional patterns.
- Patterns over loop guard variables. These summarise ranges and values that the loop guard variable can assume.
- Variables that are always powers of two. These are useful in kernels that perform tree reductions or prefix sums [49], where the variable is used as an offset for issuing reads and writes and to disable threads that no longer take part in the calculation. Sometimes it is necessary to discover relationships between a pair of power-of-two variables, e.g. that one is incrementing and the other is decrementing in lock step.
- No accesses can be in-flight when the loop head is executed. These make judgements concerning reads or writes issued during the execution of a loop.
- Uniformity of variables across threads. These are needed to verify absence of barrier divergence. They guess that threads have the same control flow or variables have the same value at the loop head.

We now give a brief description of each rule and, where possible, a motivating kernel. In the following, we assume w is an arbitrary write access of the thread to the array `out`, C is a constant value and e is an expression.

A.1 r0. accessBreak

Given an access pattern involving thread *components* (thread or block identifiers) the rule attempts to break the access pattern into its component forms using rewriting. This rule uses the intuition that relating the access pattern of a thread to into its components is useful because distinct threads must always have at least one component that is distinct.

A.2 r1. accessedOffsetsSatisfyPredicates

This rule identifies stride patterns and strength reduction loops. In the following loop, the rule will generate $w\%\texttt{blockDim.x} = \texttt{threadIdx.x}$.

```
for (int i=0; i<4; i++) {
  out[i*blockDim.x+threadIdx.x] = ...
}
```

A.3 r2. accessLowerBoundBlock and r3. accessUpperBoundBlock

These rules are analogous to accessedOffsetInRangeCTimesId, except they generate candidates when the access expression uses block indexes. In the following loop:

```
for (int i=0; i<4; i++) {
  out[C*blockDim.x+i] = ...
}
```

the rule will generate $\texttt{C*blockIdx.x} \leq w$ and $w < \texttt{C*(blockIdx.x+1)} \leq w$.

A.4 r4. accessOnlyIfEnabledInEnclosingScopes

The rule guesses that accesses can only have been issued if a thread is enabled in all enclosing scopes. For example, for the following code block:

```
if (x < k) {
  if (y < l)
    for (...)
      ...
}
```

the rule will generate $\texttt{write(out)} \Rightarrow \texttt{x} < \texttt{k} \;\&\&\; \texttt{y} < \texttt{l}$.

A.5 r5. conditionsImplyingEnabledness

The rule guesses that a thread is only enabled when it is enabled in all enclosing scopes.

A.6 r6. disabledMaintainsInstrumentation

This rule guesses that if a thread is disabled during execution of a region of code, the accesses that are being tracked for the thread cannot change as a result of this execution.

A.7 r7. guardMinusInitialIsUniform

This rule guesses that loops containing barriers must have uniform guard variables. This is based on the intuition that barrier divergence will occur otherwise. In the following loop, the rule will generate `uniform(`$x -$ `threadIdx.x)`.

```
for (i=threadIdx.x; ...) {
  __syncthreads();
}
```

A.8 r8. guardNonNeg

This rule guesses that every guard variable is non-negative. In the following loop, the rule will generate $0 \leq i$.

```
for (i=C; i>0; i--) {
  ...
}
```

A.9 r9. loopBound

This rule guesses that the initial value of a guard variable bounds the range of the guard. In the following loop, the rule will generate $e \leq i$ and $i \leq e$.

```
for (i=e; ...) {
  ...
}
```

A.10 r10. loopCounterIsStrided

This rule is analogous to accessedOffsetsSatisfyPredicates for guard variables.

A.11 r11. loopPredicateEquality

This rule is concerned with barrier divergence and uniformity of control flow.

A.12 r12. noread and r13. nowrite

These rules determine if no accesses can be in-flight when the loop head is executed due to a synchronisation appearing within the loop. In the following loop, the rule will generate `no_read(out)` and `no_write(out)`.

```
for (...) {
  __syncthreads();
}
```

A.13 r14. pow2 and r15. pow2NotZero

These rules identify possible variables that power-of-two values. This is based on the intuition that power-of-two values are often used as bit masks, tree reductions and prefix sums [49]. In the following loop, the rule will generate $x == 0 || x == 1 || ... || x == 2^{15}$.

```
for (x = N; x>0; x>>=1) {
  ...
}
```

A.14 r16. predicatedEquality

This rule is concerned with barrier divergence and uniformity of variables.

A.15 r17. relationalPow2

This rule identifies possible pairs of power-of-two variables such than one is incrementing and the other is decrementing. It then guesses a lock-step relation between them.

A.16 r18. sameWarpNoaccess

This rule concerns threads that are in the same *warp*—a unit of typically 32 threads that, on NVIDIA architectures, execute in lock step. GPUVerify provides optional support for warps [38]. If this support is enabled, this rule speculates that if the two threads under consideration are in the same warp, then neither thread has any pending accesses to the shared state (lock step execution guarantees that the threads synchronise with one another after each instruction).

REFERENCES

[1] R. W. Floyd, "Assigning meanings to programs," *Mathematical aspects of computer science*, vol. 19, no. 1, pp. 19–32, 1967.

[2] A. Gupta and A. Rybalchenko, "Invgen: An efficient invariant generator," in *CAV*, 2009, pp. 634–640.

[3] L. Kovács and A. Voronkov, "Finding loop invariants for programs over arrays using a theorem prover," in *FASE*, 2009, pp. 470–485.

[4] P. Cousot and R. Cousot, "Abstract interpretation: A unified lattice model for static analysis of programs by construction or approximation of fixpoints," in *POPL*, 1977, pp. 238–252.

[5] C. Flanagan and K. R. M. Leino, "Houdini, an annotation assistant for ESC/Java," in *FME*, 2001, pp. 500–517.

[6] C. A. J. van Eijk, "Sequential equivalence checking without state space traversal," in *DATE*, 1998, pp. 618–623.

[7] B. Jeannet and A. Miné, "Apron: A library of numerical abstract domains for static analysis," in *CAV*, 2009, pp. 661–667.

[8] A. Thakur, A. Lal, J. Lim, and T. Reps, "PostHat and all that: Automating abstract interpretation," in *TAPAS*, 2013, pp. 15–32.

[9] K. L. McMillan, "Lazy abstraction with interpolants," in *CAV*, 2006, pp. 123–136.

[10] I. Dillig, T. Dillig, B. Li, and K. McMillan, "Inductive invariant generation via abductive inference," in *OOPSLA*, 2013, pp. 443–456.

[11] B. Jeannet, P. Schrammel, and S. Sankaranarayanan, "Abstract acceleration of general linear loops," in *POPL*, 2014, pp. 529–540.

[12] M. D. Ernst, J. Cockrell, W. G. Griswold, and D. Notkin, "Dynamically discovering likely program invariants to support program evolution," *IEEE Trans. Software Eng.*, vol. 27, no. 2, pp. 99–123, 2001.

[13] C. Flanagan, R. Joshi, and K. R. M. Leino, "Annotation inference for modular checkers," *Inf. Process. Lett.*, vol. 77, no. 2–4, pp. 97–108, 2001.

[14] A. Betts, N. Chong, A. F. Donaldson, S. Qadeer, and P. Thomson, "GPUVerify: a verifier for GPU kernels," in *OOPSLA*, 2012, pp. 113–132.

[15] T. Mytkowicz, A. Diwan, M. Hauswirth, and P. F. Sweeney, "Producing wrong data without doing anything obviously wrong!" in *ASPLOS*, 2009, pp. 265–276.

[16] NVIDIA, "CUDA C programming guide, version 5.5," 2013.

[17] Khronos OpenCL Working Group, "The OpenCL specification, version 2.0," 2013.

[18] P. Collingbourne, A. F. Donaldson, J. Ketema, and S. Qadeer, "Interleaving and lock-step semantics for analysis and verification of GPU kernels," in *ESOP*, 2013, pp. 270–289.

[19] A. Betts, N. Chong, A. F. Donaldson, J. Ketema, S. Qadeer, P. Thomson, and J. Wickerson, "The design and implementation of a verification technique for GPU kernels," *ACM Trans. Program. Lang. Syst.*, vol. 37, no. 3, p. 10, 2015.

[20] M. Barnett, B.-Y. E. Chang, R. DeLine, B. Jacobs, and K. R. M. Leino, "Boogie: A modular reusable verifier for object-oriented programs," in *FMCO*, 2005, pp. 364–387.

[21] L. M. de Moura and N. Bjørner, "Z3: An efficient SMT solver," in *TACAS*, 2008, pp. 337–340.

[22] C. Barrett, C. L. Conway, M. Deters, L. Hadarean, D. Jovanović, T. King, A. Reynolds, and C. Tinelli, "CVC4," in *CAV*, 2011, pp. 171–177.

[23] M. Barnett and K. R. M. Leino, "Weakest-precondition of unstructured programs," in *PASTE*, 2005, pp. 82–87.

[24] AMD, "Accelerated Parallel Processing SDK," accessed 2014, http://developer.amd.com/sdks/amdappsdk.

[25] NVIDIA, "GPU Computing SDK," accessed 2014, https://developer.nvidia.com/gpu-computing-sdk.

[26] Microsoft Corporation, "C++ AMP sample projects for download (MSDN blog)," accessed 2014, http://blogs.msdn.com/b/nativeconcurrency/archive/2012/01/30/c-amp-sample-projects-for-download.aspx.

[27] A. Bakhoda, G. L. Yuan, W. W. L. Fung, H. Wong, and T. M. Aamodt, "Analyzing CUDA workloads using a detailed GPU simulator," in *ISPASS*, 2009, pp. 163–174.

[28] J. A. Stratton, C. Rodrigues, I.-J. Sung, N. Obeid, L.-W. Chang, N. Anssari, G. D. Liu, and W. mei W. Hwu, "Parboil: A revised benchmark suite for scientific and commercial throughput computing," UIUC, Tech. Rep. IMPACT-12-01, 2012.

[29] S. Che, J. W. Sheaffer, S.-H. Lee, and K. Skadron, "Rodinia: A benchmark suite for heterogeneous computing," in *Workload Characterization*, 2009, pp. 44–54.

[30] A. Danalis, G. Marin, C. McCurdy, J. S. Meredith, P. C. Roth, K. Spafford, V. Tipparaju, and J. S. Vetter, "The scalable heterogeneous computing (SHOC) benchmark suite," in *GPGPU*, 2010, pp. 63–74.

[31] S. Verdoolaege, J. C. Juega, A. Cohen, J. I. Gómez, C. Tenllado, and F. Catthoor, "Polyhedral parallel code generation for CUDA," *ACM Trans. Arch. Code Opt.*, vol. 9, no. 4, p. 54, 2013.

[32] L.-N. Pouchet, "PolyPench/C: The polyhedral benchmark suite," accessed 2015, http://www.cs.ucla.edu/~pouchet/software/polybench/.

[33] Rightware Oy, "Basemark CL," accessed 2014, http://www.rightware.com/basemark-cl/.

[34] N. Chong, A. F. Donaldson, P. Kelly, J. Ketema, and S. Qadeer, "Barrier invariants: a shared state abstraction for the analysis of data-dependent GPU kernels," in *OOPSLA*, 2013, pp. 605–622.

[35] E. Bardsley, A. F. Donaldson, and J. Wickerson, "KernelInterceptor: automating GPU kernel verification by intercepting and generalising kernel parameters," in *IWOCL*, 2014.

[36] R. Baghdadi, U. Beaugnon, A. Cohen, T. Grosser, M. Kruse, C. Reddy, S. Verdoolaege, A. Betts, A. F. Donaldson, J. Ketema, J. Absar, S. van Haastregt, A. Kravets, A. Lokhmotov, R. Dávid, and E. Hajiyev, "PENCIL: A platform-neutral compute intermediate language for accelerator programming," in *PACT*, 2015, pp. 138–149.

[37] A. F. Donaldson, J. Ketema, and S. Verdoolaege, "Translation validation for the PENCIL → OpenCL compiler," 2014, Chapter 5 of CARP project deliverable D6.4, http://carp.doc.ic.ac.uk/external/publications/D6.4.pdf.

[38] E. Barsdley and A. F. Donaldson, "Warps and atomics: Beyond barrier synchronisation in the verification of GPU kernels," in *NFM*, 2014.

[39] E. M. Clarke, D. Kroening, and F. Lerda, "A tool for checking ANSI-C programs," in *TACAS*, 2004, pp. 168–176.

[40] N. Polikarpova, C. A. Furia, and S. West, "To Run What No One Has Run Before: Executing an Intermediate Verification Language," in *RV*, 2013, pp. 251–268.

[41] D. Liew, C. Cadar, and A. F. Donaldson, "Symbooglix: A symbolic execution engine for Boogie programs," in *ICST*, 2016, pp. 45–56.

[42] P. Jaccard, "The distribution of the flora in the alpine zone," *New Phytologist*, vol. 11, no. 2, pp. 37–50, 1912.

[43] C. Flanagan, R. Joshi, and K. R. M. Leino, "Annotation inference for modular checkers," *Inf. Process. Lett.*, vol. 77, no. 2–4, pp. 97–108, 2001.

[44] S. Graf and H. Saïdi, "Construction of abstract state graphs with PVS," in *CAV*, 1997, pp. 72–83.

[45] A. Lal, S. Qadeer, and S. K. Lahiri, "A solver for reachability modulo theories," in *CAV*, 2012, pp. 427–443.

[46] T. Ball, A. Podelski, and S. K. Rajamani, "Boolean and cartesian abstraction for model checking C programs," *STTT*, vol. 5, no. 1, pp. 49–58, 2003.

[47] J. W. Nimmer and M. D. Ernst, "Invariant inference for static checking," in *FSE*, 2002, pp. 11–20.

[48] N. Polikarpova, I. Ciupa, and B. Meyer, "A comparative study of programmer-written and automatically inferred contracts," in *ISSTA*, 2009, pp. 93–104.

[49] G. E. Blelloch, "Prefix sums and their applications," in *Synthesis of Parallel Algorithms*. Morgan Kaufmann, 1990.